

Accessing Cationic α -Silylated and α -Germylated Phosphorus Ylides

Felix Krämer,^[a] Michael Radius,^[a] Alexander Hinz,^[a] Melina E. A. Dilanas,^[a] and Frank Breher^{*[a]}

Dedicated to Prof. Holger Braunschweig on the occasion of his 60th birthday.

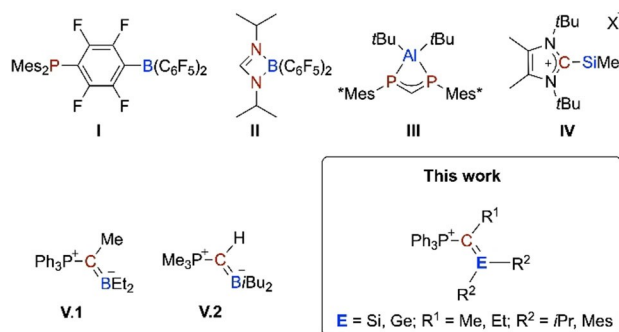
Abstract: The synthesis and full characterization of α -silylated (α -SiCPs; **1–7**) and α -germylated (α -GeCPs; **11–13**) phosphorus ylides bearing one chloride substituent $R_3PC(R^1)E(Cl)R^2$ ($R = Ph$; $R^1 = Me, Et, Ph$; $R^2 = Me, Et, iPr, Mes$; $E = Si, Ge$) is presented. The molecular structures were determined by X-ray diffraction studies. The title compounds were applied in halide abstraction studies in order to access cationic species. The reaction of $Ph_3PC(Me)Si(Cl)Me_2$ (**1**) with $Na[B(C_6F_5)_4]$ furnished the dimeric phosphonium-like dication $[Ph_3PC(Me)SiMe_2]_2[B(C_6F_5)_4]_2$ (**8**). The highly reactive, mesityl- or *i*Pr-substituted cationic species $[Ph_3PC(Me)SiMes_2][B(C_6F_5)_4]$ (**9**) and $[Ph_3PC(Et)SiPr_2][B(C_6F_5)_4]$ (**10**) could be characterized by NMR spectroscopy. Carrying out the halide abstraction

reaction in the sterically demanding ether *i*Pr₂O afforded the protonated α -SiCP $[Ph_3PCH(Et)Si(Cl)iPr_2][B(C_6F_5)_4]$ (**6 dec**) by sodium-mediated basic ether decomposition, whereas successfully synthesized $[Ph_3PC(Et)SiPr_2][B(C_6F_5)_4]$ (**10**) readily cleaves the F–C bond in fluorobenzene. Thus, the ambiphilic character of α -SiCPs is clearly demonstrated. The less reactive germanium analogue $[Ph_3PC(Me)GeMes_2][B\{3,5-(CF_3)_2C_6H_3\}_4]$ (**14**) was obtained by treating **11** with $Na[B\{3,5-(CF_3)_2C_6H_3\}_4]$ and fully characterized including by X-ray diffraction analysis. Structural parameters indicate a strong $C_{ylide}-Ge$ interaction with high double bond character, and consequently the C–E ($E = Si, Ge$) bonds in **9**, **10** and **14** were analyzed with NBO and AIM methods.

Introduction

Frustrated Lewis pairs (FLPs) have been studied in great detail in recent years.^[1] Most commonly, a combination of a sterically hindered Lewis acid and a Lewis base are applied, leading to “frustration” by preventing Lewis acid/base adduct formation. The majority of known FLP systems use group 13 element-based Lewis acids with electron-withdrawing substituents in order to increase the Lewis acidity, as in the landmark example **I** (Scheme 1) by the Stephan group.^[1f] Phosphine and amine derivatives are the most common Lewis basic counterparts. Combination of stronger Lewis acidic cationic silicon compounds and phosphines or amines is much less common.^[2]

Moreover, so-called hidden FLPs were reported,^[3] which seem to be not frustrated at first glance, as a bond between acidic and basic site is formed. However, ring strain or steric strain can still enable dissociation of the acidic and basic site



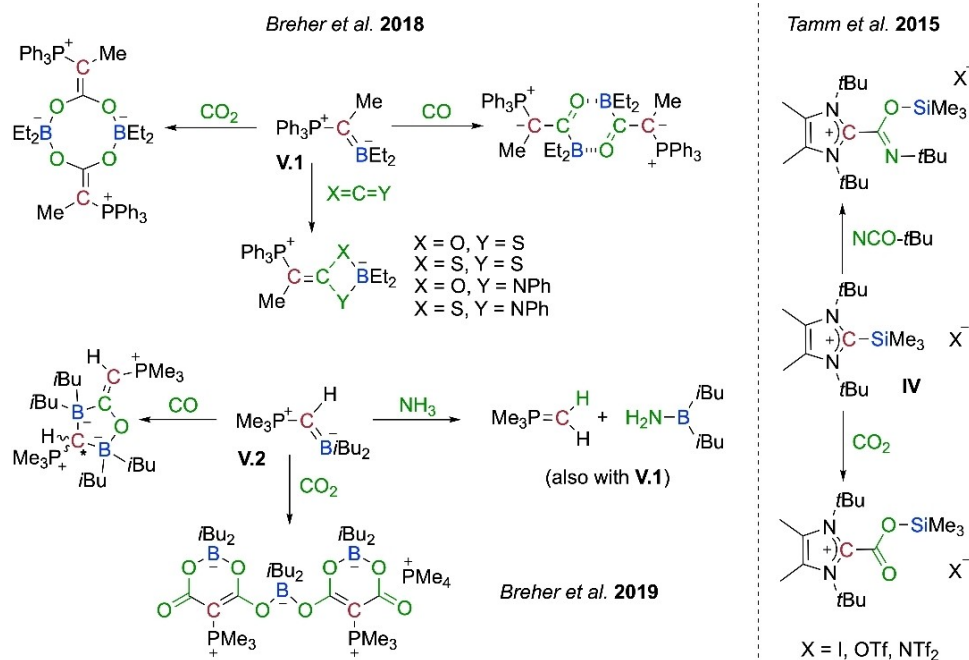
Scheme 1. Selected examples of FLPs, hidden FLPs and ambiphilic ylides.

and promote the reaction towards small molecules such as H₂, CO or CO₂. Examples of such hidden FLPs have been reported, for example, by Stephan’s and our groups (**II** and **III**),^[3b,e] and the only FLP combining a C-based Lewis base with a cationic silicon-based Lewis acid was published by Tamm and co-workers (**IV**).^[4] Our group recently reported electronic frustration in α -borylated phosphorus ylide (α -BCPs) featuring a highly polarized borataalkene unit (Scheme 1, **V.1** and **V.2**). We showed that these α -BCPs readily react with NH₃, CO, CO₂ and other heteroallenes (Scheme 2, left).^[5] This reactivity is closely related to the reactivity of the cationic carbene adduct $[tBu-SiMe_3]Cl$ (**IV**, $tBu = (MeCN\{tBu\})_2C$), which shows FLP-type reactivity towards NCOtBu and CO₂ (Scheme 2, right). Therefore, it is indeed possible to generate electronic frustration or at least a very reactive, highly polarized^[6] C/B π -bond by competition

[a] F. Krämer, Dr. M. Radius, Dr. A. Hinz, M. E. A. Dilanas, Prof. Dr. F. Breher
Karlsruhe Institute of Technology (KIT)
Institute of Inorganic Chemistry, Division Molecular Chemistry
Engesserstraße 15, 76131 Karlsruhe (Germany)
E-mail: breher@kit.edu
Homepage: <https://www.aoc.kit.edu/breher/index.php>

Supporting information for this article is available on the WWW under <https://doi.org/10.1002/chem.202103974>

© 2021 The Authors. Chemistry - A European Journal published by Wiley-VCH GmbH. This is an open access article under the terms of the Creative Commons Attribution Non-Commercial License, which permits use, distribution and reproduction in any medium, provided the original work is properly cited and is not used for commercial purposes.



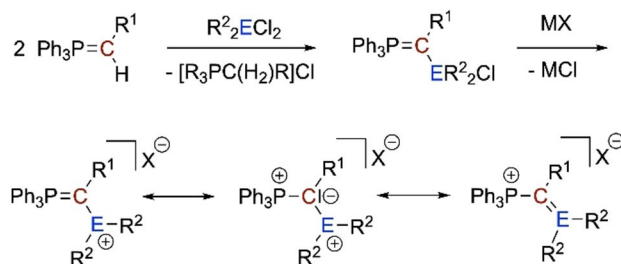
Scheme 2. Reactivity of the α -BCPs V.1 and V.2 (left) and the cationic carbene adduct IV (right) towards small molecules.

for the electron pair on the Lewis basic carbon center. In order to further extend our activities in this area, we intended to access cationic α -silylated and α -germylated phosphorus ylides (Scheme 1).

π -Stabilized silicon cations are of fundamental interest. Komatsu published the first π -stabilized silylium ion in 2000, which, however, could only be characterized in solution.^[7] Greb and co-workers recently reported on a dimeric tris(dimethylamino) silylium cation.^[8] A surprisingly high fluoride ion affinity (FIA) of 809.6 kJ mol⁻¹ for the hypothetical monomer was reported. The Lewis acidity of silicon and germanium cations^[9] as well as their versatile chemistry has been well examined.^[9a,b,10] Gessner and co-workers recently reported on stabilized ylide-substituted dinuclear cationic germanium analogue of a vinyl cation [Ph₃PC(TolSO₂)Ge]₂[SnCl₃], which can be described as germylene stabilized Ge^{II} cation.^[11] Nonstabilized phosphorus ylide-substituted silicon and germanium cations are, to the best of our knowledge, not yet known in the literature,^[10e,12,13] but their reactivity can be expected to resemble that of the highly reactive C=E (E=Si, Ge) double bonds in silenes and germenes.^[14] Herein we report on the syntheses and characterization of new α -silylated and germyleated phosphorus ylides bearing one chloride substituent on the group 14 element, including studies on cation formation by halide abstraction (Scheme 3).

Results and Discussion

α -Substituted phosphorus ylides are readily available by *trans*-ylidation (Scheme 3).^[5a,15] Thus, our synthetic strategy to α -silylated (α -SiCPs) and α -germylated (α -GeCPs) phosphorus

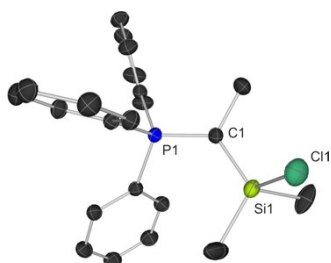


Scheme 3. Reaction scheme for the synthesis of α -Si/GeCPs and their cationic analogues, including possible resonance structures (R¹ = Me, Et, Ph; R² = Me, Et, *i*Pr, Mes; E = Si, Ge; MX = Na[B(C₆F₅)₄]).

ylides followed this route. Three different groups R¹ (R¹ = Me, Et, Ph) were chosen as substituent for the ylidic carbon atom due to the ready availability of the corresponding starting materials. The phosphonium salts [Ph₃PC(R¹)H]₂Br were straightforwardly converted to the ylides Ph₃PC(R¹)H by deprotonation.^[16] Subsequent treatment of the ylides with dichlorosilanes in a 2:1 stoichiometric ratio resulted in *trans*-ylidation and formation of the silylated phosphorus ylides 1–7. In these novel phosphorus ylides, the substituents on the heavier tetrels R² were either Me, Et, *i*Pr or Mes to study effects of steric strain (Table 1). These reactions for the synthesis of 1–7 were carried out in toluene followed by filtration and extraction with boiling hexane (reaction conditions and yields for 1–7 are given in Table 4 in the Experimental Section). Crystals suitable for X-ray analysis were obtained by recrystallization from hexane. The crystal structure of 1 is exemplarily shown in Figure 1 (crystal structures of 2–7 and all other crystallographic parameters are

Table 1. Selected bond lengths [Å] and angles [°] of 1–7.

	R on C _{Ylide} (R ¹)	R on Si (R ²)	P1–C1 [Å]	C1–Si1 [Å]	P1–C1–Si1 [°]
1	Me	Me	1.689(1)	1.793(1)	123.32(7)
2	Me	Et	1.682(2)	1.786(2)	127.4(1)
3	Me	Mes	1.699(3)	1.785(3)	127.4(2)
4	Et	Me	1.683(2)	1.807(2)	121.2(1)
5	Et	Et	1.690(2)	1.802(2)	122.29(9)
6	Et	<i>i</i> Pr	1.692(3)	1.803(3)	127.1(2)
7	Ph	Me	1.693(2)	1.795(2)	125.90(8)

**Figure 1.** Molecular structure of 1; ellipsoids are drawn at the 30% probability level. Hydrogen atoms are omitted for clarity. Selected distances [Å] and angles [°]: P1–C1 = 1.6891(12); C1–Si1 = 1.7930(13) and P1–C1–Si1 = 123.32(7).

given in Section S3 in the Supporting Information). Selected bond lengths and angles of 1–7 are shown in Table 1.

The P1–C1 bonds in 1–7 are 2–3 pm shorter than the bond in Ph₃PC(Me)BEt₂ (**V.1**, 1.717(3) Å), which can be attributed to less delocalization of the π-electron density towards the α* acceptor orbitals of the Si moiety compared to the {BEt₂} fragment featuring a proper π-acceptor orbital.^[5a] The C1–Si1 bonds are noticeably shorter (8–10 pm) than the calculated average C–Si single bond radii of 1.88 Å;^[17] this can be attributed to ionic contributions or to hyperconjugative effects.^[18] The angles P1–C1–Si1 are 1–7° wider than the ideal angle on sp² carbon atoms of 120°.

Back in 1991, Grützmacher and co-workers showed that cationic α-stannylum ylides ([Ph₃PC(H)SnBu₂]⁺[BF₄][−]) tend to dimerize.^[19] Prior to employing the starting materials 1–7 in halide abstraction reaction in order to generate cationic α-silylium ylides (denoted α-Si+CPs hereafter), DFT calculations at the TPSS/def2-TZVP level of theory including D3BJ dispersion correction were performed. The dimerization energies of eleven potential cationic α-Si+CPs were investigated and the results are compiled in Table 2.

As expected, the dimerization energies strongly depend on the substituent pattern. For the model compound [Ph₃PC(Me)SiMe₂]⁺ (entry 1) featuring small substituents on both the ylidic carbon atom (R¹) and the silicon center (R²) the dimer is favored by 112 kJ mol^{−1}. Upon increasing the steric bulk to R¹/R² = Et/Et (entry 2), Ph/Me (entry 3) and Ph/Et (entry 4), the dimer becomes increasingly disfavored. Once *iso*-propyl groups are considered as R² on the silicon center (entries 6–8) values of +32 (R¹ = Me), +99 (R¹ = Et), and +105 kJ mol^{−1} (R¹ = Ph) are calculated, indicating that the monomeric species become energetically favored. Based on these calculations, *i*Pr-substi-

Table 2. Calculated dimerization energies of potential α-Si+CPs (dimer with R¹ = Me, R² = Mes could not be converged)

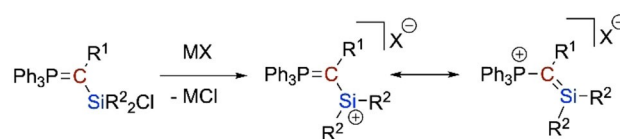
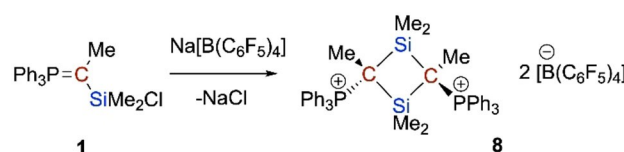
R on C _{Ylide} (R ¹)	R on Si (R ²)	ΔE [kJ mol ^{−1}]
Me	Me	−111.51
Et	Et	−92.92
Ph	Me	−70.26
Ph	Et	−22.49
Ph	Ph	+3.80
Me	<i>i</i> Pr	+32.39
Et	<i>i</i> Pr	+98.88
Ph	<i>i</i> Pr	+104.57
Me	Mes	−
Mes	Me	+113.49
Mes	Et	+145.59

tuted starting materials should possess a great potential for the synthesis of monomeric silylium ions. We noted that even more positive values of up to +113–146 kJ mol^{−1} could be obtained for the R¹/R² combinations Mes/Me and Mes/Et, that is, with a mesityl group on the ylidic carbon atom. However, all attempts to synthesize α-SiCPs possessing a mesityl substituent at the α-carbon atom by *trans*-ylation lead to decomposition of the reaction mixtures. Towards dehydrohalogenation with metal bases like Na[N(SiMe₃)₂], 1:1 mixtures of Ph₃PC(H)Mes and R₂SiCl₂ (R = Me, Et) showed no reactivity. The phenyl-substituted ylide Ph₃PC(H)Ph showed similar behavior with R₂SiCl₂ (R = *i*Pr).

Studies on cation formation by chloride abstraction

Halide abstraction, besides hydride^[10b] or allyl group^[10d] abstraction, is a well-established synthetic route to silylium cations. Different sodium and silver salts of weakly coordinating anions (WCAs) were tested (Scheme 4).

Initially, all reactions were carried out in benzene or toluene to prevent reaction of the cationic species with the solvent. Reaction of **1** with Na[B(C₆F₅)₄] in toluene leads to the dimeric “phosphonium-like” dication **8** (Scheme 5). Studies in solution

**Scheme 4.** Reaction scheme to cationic α-Si+CPs (R¹ = Me, Et, Ph; R² = Me, Et, *i*Pr, Mes; M⁺ = Na⁺, Ag⁺; X[−] = OTf[−], [BF₄][−], [PF₆][−], [SbF₆][−], [BPh₄][−], [B(C₆F₅)₄][−], [Al{OC(CF₃)₃]₄[−]).**Scheme 5.** Synthesis of the dimeric diphosphonium dication **8**.

showed that **8** consists of *trans* and *cis* isomers in the ratio 1.7:1.

Crystals suitable for X-ray diffraction were obtained by slow concentration of a methylene chloride solution of **8** (Figure 2).

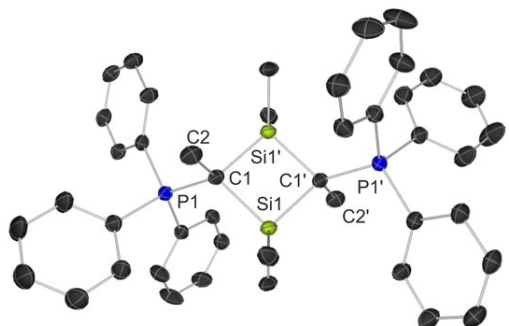
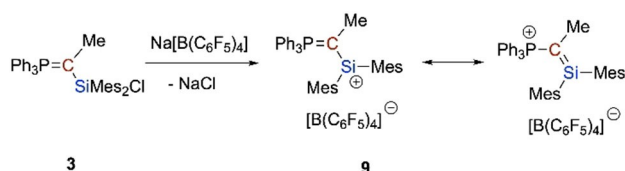


Figure 2. Molecular structure of **8**; ellipsoids are drawn at the 30% probability level. Only the cationic part is shown; hydrogen atoms are omitted for clarity. Selected distances [Å] and angles [°]: P1–C1 = 1.8070(14); Si1–C1 = 1.9545(16); C1–Si1–C1 = 90.88(6); P1–C1–Si1 = 119.73(8); C2–C1–P1 = 106.96(11); C2–C1–Si1 = 107.92(10).



Scheme 6. Synthesis of **9** in benzene at RT.

The P1–C1 bond in **8** is elongated by 11 pm compared to **1** indicating less double bond character. The angles C2–C1–P1 = 106.96(11)° and C2–C1–Si1 = 107.92(10)° are very close to the ideal tetrahedral angle (109°), which clearly indicates an sp³-hybridized carbon center. In contrast, the angle P1–C1–Si1 of 119.73(8)° is relatively obtuse due to the steric demand of the PPh₃ moieties. The Si1–C1 bond is elongated by 6 pm compared to the calculated Si–C bond length of 1.89 Å based on single bond radii.^[17]

Because of the poor solubility of the oily reaction products in aromatic solvents after chloride abstraction with Na[B(C₆F₅)₄], a series of sodium salts with other WCAs were checked in order to increase the solubility. **7** showed no reaction towards NaX (X[−] = [PF₆][−], [BF₄][−], [SbF₆][−], [BPh₄][−], and OTf[−]) in benzene, even at 90 °C for 24 h. The reaction of **7** with Ag[Al{OC(CF₃)₃}]₄ resulted in a deep purple, insoluble oil and elementary metal, indicating a redox reaction instead of halide abstraction. Due to the poor solubility, further synthesis was carried out in CH₂Cl₂ or THF. It quickly turned out that **8** represents the only isolable compound under these conditions and that **2**, **4**, **5** and **7** readily decompose to [Ph₃PC(R)H₂][B(C₆F₅)₄]. Even *ortho*-dichlorobenzene (*o*-DCB), which is a common solvent in silicon cation chemistry,^[10f] showed poor stability towards intermediary formed cationic species. This underlines the amphiphilic character and high reactivity of the cationic α-Si+CPs. Nevertheless, reaction of **3** with Na[B(C₆F₅)₄] in benzene leads to discoloration of the formerly yellow solution (Scheme 6).

Although the cationic compound [Ph₃PC(Me)SiMes₂][B(C₆F₅)₄] (**9**) could not be crystallized or isolated due to decomposition, we found clear indications for its formation by NMR spectroscopy (Figure 3). Due to poor solubility of the salt,

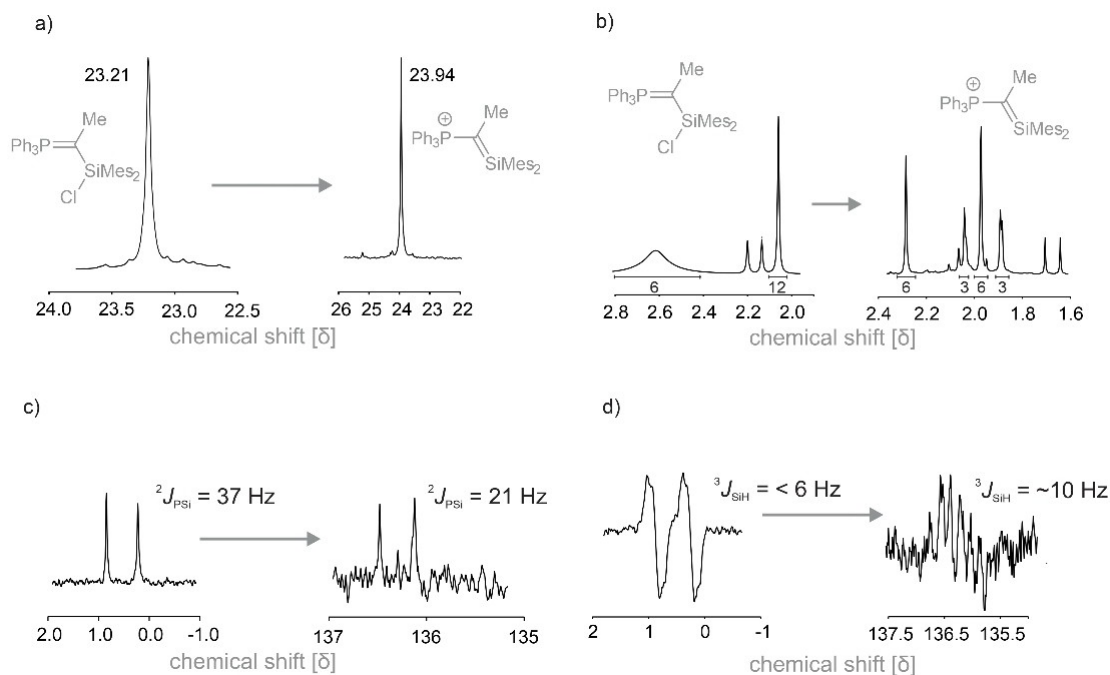


Figure 3. Detected ¹H, ³¹P{¹H}, ²⁹Si, and ²⁹Si{¹H} NMR resonances of **3** and **9**: a) downfield shifting of the ³¹P{¹H} NMR resonance; b) hindered rotation of the Si–C_{vide} bond; c) downfield shifting of the ²⁹Si NMR resonance (INEPTD) and reduction of the ²J(P,Si) coupling; d) stronger ³J(Si,H) coupling (INEPTND).

a mixture of benzene and fluorobenzene (4:1) was used. In the $^{31}\text{P}\{^1\text{H}\}$ NMR spectra (Figure 3a), an expected downfield shift of +0.7 ppm could be detected, indicating the more electron-withdrawing nature of the cationic $\{\text{SiMe}_2\}$ fragment (as compared to $\{\text{SiMe}_2\text{Cl}\}$ in **3**). Furthermore, the α -BCP $\text{Ph}_3\text{PC}(\text{Me})\text{BEt}_2$ (**V.1**) showed hindered rotation of the $\text{C}_{\text{ylide}}\text{--B}$ bond caused by double bond character leading to discrete NMR resonances for the ethyl groups of the $\{\text{BEt}_2\}$ entity.^[5a] In the ^1H NMR spectra of **3**, a broad signal for the *ortho*-methyl groups of the mesityl substituent were detected (Figure 3b). Formation of the cation **9** results in clear separation of mesityl group resonances. ^{29}Si NMR measurements were performed using INEPTD (no proton coupling) and INEPTND (with proton coupling) protocols. The INEPTD experiments (Figure 3c) show that the $^2J_{\text{PSi}}$ coupling constant of 21 Hz for **9** is considerably smaller as compared to **3** (37 Hz). This may be caused by the reduction of ylene character. Also, the $^3J_{\text{PH}}$ coupling constant of the phosphorus atom to the ylidic CH_3 group decreases from 19.5 to 19 Hz, while the $^3J_{\text{SiH}}$ coupling constant simultaneously increases. In the ^1H NMR spectrum of **9**, silicon satellites with a coupling constant of 10.5 Hz were observed, which are not observed in the ^1H NMR spectra of **3** (below 6 Hz baseline of the signal). This Si–H J coupling is also observed in the ^{29}Si INEPTND experiments (Figure 3d). In the ^{29}Si NMR spectra, one signal at $\delta(^{29}\text{Si}) = 136.3$ ppm could be detected. The free silylium cation Me_3Si^+ shows a ^{29}Si NMR chemical shift of $\delta(^{29}\text{Si}) = 225.5$ ppm.^[10c] Such a strong downfield shifting is not expected for **9** due to the electron density provided by the ylide substituent. The π -conjugated silylium ion of Komatsu displays a more similar electronic situation to α -Si+CP and, correspondingly, its ^{29}Si NMR shift was observed at $\delta(^{29}\text{Si}) = 142.9$ ppm.^[7] In addition, DFT calculations at the TPSS/TZVP level of theory for the chemical shielding of **9** were performed. The calculated ^{29}Si NMR shift for the α -Si+CP of $\delta(^{29}\text{Si})_{\text{calc.}} = 141$ ppm is in good agreement with experimental findings.

Furthermore, the fluoride ion affinity (FIA)^[9c] including solvent correction (FIA_{solv}) of **9** was calculated (TPSS/TZVP) towards the isodesmic reaction of the $\text{Me}_3\text{Si}^+/\text{Me}_3\text{SiF}$ system (further details are given in Section S4). The FIA of 691 kJ mol^{-1} ($\text{FIA}_{\text{solv}} = 589$ kJ mol^{-1}) is significantly higher compared to isoelectronic α -BCP $\text{Ph}_3\text{PC}(\text{H})\text{B}(\text{C}_6\text{F}_5)_2$ (**qB**, 271 kJ mol^{-1} ; $\text{FIA}_{\text{solv}} = 225$ kJ mol^{-1}) and the hypothetical aluminium analogue $\text{Ph}_3\text{PC}(\text{Me})\text{AlMe}_2$ (**qAl**, 360 kJ mol^{-1} ; $\text{FIA}_{\text{solv}} = 256$ kJ mol^{-1} ; Figure 4).

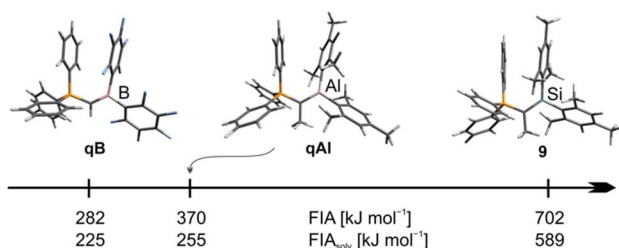
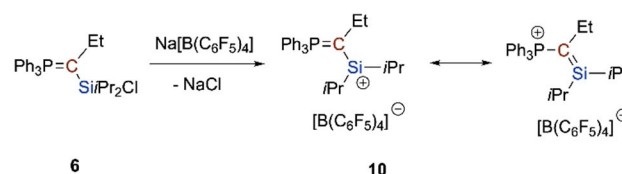


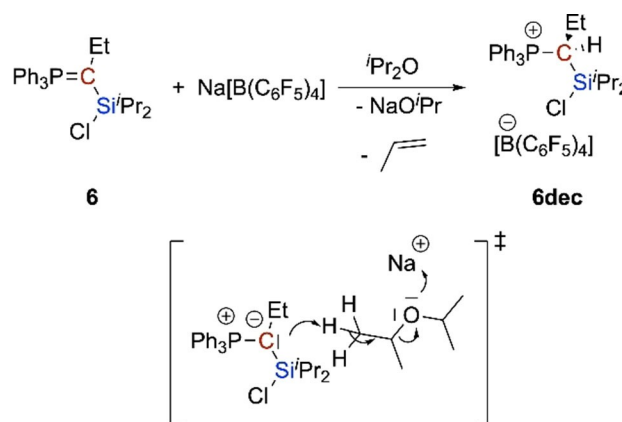
Figure 4. Comparison of the FIAs of **9** with its isoelectronic analogues **qB** and **qAl**.

Still higher FIA of 735 kJ mol^{-1} ($\text{FIA}_{\text{solv}} = 659$ kJ mol^{-1}) was obtained by changing the substituent pattern at the silicon center from aromatic to aliphatic ($\text{R}^1 = \text{Et}$, $\text{R}^2 = i\text{Pr}$). The reaction of **6** with $\text{Na}[\text{B}(\text{C}_6\text{F}_5)_4]$ in benzene results in the formation of an insoluble yellow oil (Scheme 7) that could not be purified or crystallized. Unlike **9**, the formed cationic species **10** undergoes decomposition when adding PhF , which is consistent with the large calculated FIA. In order to record NMR spectra of the insoluble oily residue, it was layered with perfluorohexane to position the sample at the correct level of the measurement window. For internal reference, a capillary with C_6D_6 was inserted (Figure S39). The ^{29}Si and ^{31}P NMR spectra obtained in this way clearly indicated the formation of the cation $[\text{Ph}_3\text{PC}(\text{Et})\text{Si}i\text{Pr}_2][\text{B}(\text{C}_6\text{F}_5)_4]$ (**10**). The ^{29}Si NMR resonance at $\delta(^{29}\text{Si}) = 164.3$ ppm is shifted downfield by 28 ppm with respect to **9**. In the $^{31}\text{P}\{^1\text{H}\}$ NMR spectra, the detected resonance at $\delta(^{31}\text{P}) = 26.8$ ppm is also shifted 3.8 ppm downfield compared to **9**. This is in good agreement with less electron-donating properties of the isopropyl groups compared to mesityl, and the accompanying higher electron-withdrawing character of the $\{\text{SiR}_2\}$ fragment. Due to the fact that the cationic species are not stable towards halogenated solvents, the sterically demanding diisopropyl ether $i\text{Pr}_2\text{O}$ was tested as potential solvent. Reaction of **6** with $\text{Na}[\text{B}(\text{C}_6\text{F}_5)_4]$ surprisingly lead to the protonated silicon ylide **6 dec** (Scheme 8).

It appears reasonable to assume that the product is formed by sodium-mediated basic ether splitting forming $\text{NaO}i\text{Pr}$ and propene.^[20] These results corroborate the amphiphilic character of silylated ylides. Colorless crystals suitable for X-ray analysis



Scheme 7. Synthesis of **10** in benzene at RT.



Scheme 8. Reaction to give the protonated silicon ylide **6 dec** and the proposed transition state of the reaction.

were obtained by recrystallization from a mixture of *i*Pr₂O and hexane (Figure 5).

The P1–C1 bond of 1.819(5) Å is elongated by 13 pm compared to **6**, which would be in line with a smaller double bond character. This is further supported by the similarity to the P1–C1 bond length in the dimer **8** (1.807 Å). Elongation of the C1–Si1 distance of 1.947(5) by 14 pm as well shortening of *d*(Si1–C4) (1.862(6) Å) and *d*(Si1–Cl1) (2.0729(19) Å) by 3 and

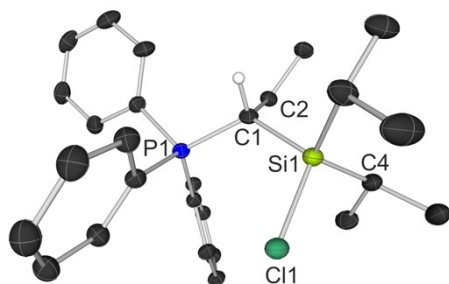
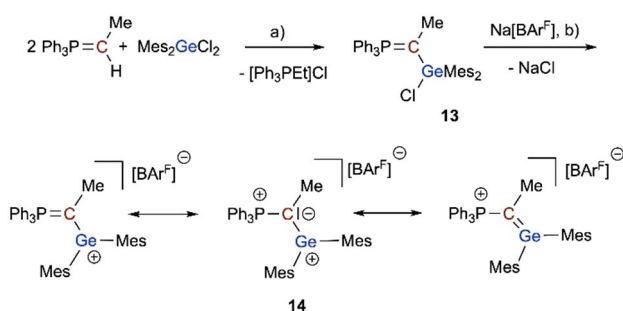


Figure 5. Molecular structure of **6 dec**; ellipsoids are drawn at the 10% probability level. Only the cationic part is shown; hydrogen atoms (except H1) are omitted for clarity. Selected distances [Å] and angles [°]: P1–C1 = 1.819(5); C1–Si1 = 1.947(5); Si1–C4 = 1.862(6); Si1–Cl1 = 2.0729(19); P1–C1–Si1 = 118.8(2).



Scheme 9. Synthesis of **14**. a) toluene, 90 °C, 2 h; b) toluene, RT.

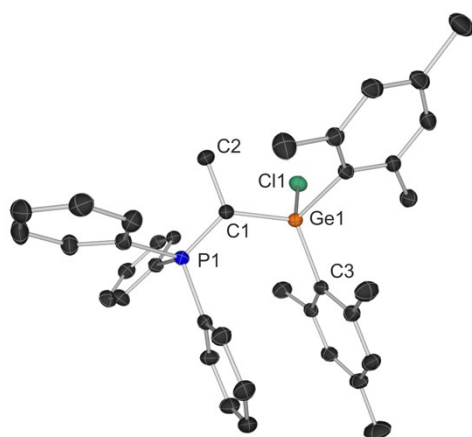


Figure 6. Molecular structure of **13**; ellipsoids are drawn at the 30% probability level. Hydrogen atoms are omitted for clarity. Selected distances [Å] and angles [°]: P1–C1 = 1.685(2); C1–Ge1 = 1.878(2); Ge1–C3 = 1.993(2); Ge1–Cl1 = 2.2615(8); C1–C2 = 1.528(3); P1–C1–Ge1 = 126.85(11).

7 pm, respectively, underline a lesser electron donation from the ylide to the silicon center.

Studies on α -germylated phosphorus ylides

After the promising generation of cationic silylium ylides, we focused on the synthesis of their germanium analogues. The starting materials **11–13** (R^1/R^2 = Me/Me (**11**), Ph/Me (**12**), Me/Mes (**13**)) were synthesized by *trans*-ylidation followed by chloride abstraction with Na[B(3,5-(CF₃)₂C₆H₃)] (NaBAr^F, Scheme 9).

Crystals of **13** obtained from concentration of a toluene solution were analyzed by X-ray diffraction (Figure 6). The distance *d*(P1–C1) of 1.685(2) Å in **13** is 1.4 pm shorter compared to the silicon analogue **3**, which indicates less stabilization of the ylide. In contrast, the Ge1–C1 bond of 1.878(2) Å is comparatively short in relation to the Ge1–C3(aryl) bond length (1.993(2) Å), indicating a strong negative hyperconjugation of electron density from the ylidic carbon to the germanium center. The additional elongation of the Ge1–Cl1 bond (2.2615(8) Å) underscores this assumption (cf. Mes₂GeCl₂ (*d*(Ge–Cl) = 2.179 Å; structural data of Mes₂GeCl₂ are shown in Section S3). The behavior of **13** in solution is quite similar to **3**. The *ortho*-methyl groups show large broadening in the ¹H NMR signals. The doublet of the ylidic methyl group at $\delta(^1\text{H})$ = 2.34 ppm possesses a coupling constant of 18.8 Hz, which was found to be slightly smaller than in **3** (19.5 Hz). The ³¹P{¹H} resonance of $\delta(^{31}\text{P})$ = 21.8 ppm is less downfield-shifted than in **3** (23.2 ppm).

The reaction of **13** with NaBAr^F in toluene followed by extraction in CH₂Cl₂ gave **14** as light yellow crystalline solid in 30% yield (Scheme 9). Crystals suitable for X-ray diffraction were obtained by slow concentration of a CH₂Cl₂ solution of **14** at room temperature (Figure 7).

The P1–C1 distance of 1.739(4) Å is elongated by 5.4 pm as compared to **13**. This indicates a weak P–C_{ylide} interaction. The germanium carbon bond length of 1.808(4) Å (C1–Ge1) is

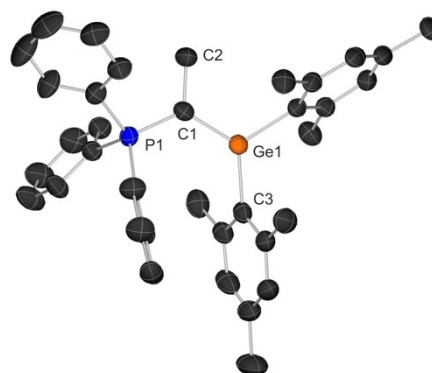


Figure 7. Molecular structure of **14**, ellipsoids are drawn at the 30% probability level. Only the cationic part is shown; hydrogen atoms are omitted for clarity. Selected distances [Å] and angles [°]: P1–C1 = 1.739(4); C1–C2 = 1.521(6); Ge1–C1 = 1.808(4); Ge1–C3 = 1.931(5); P1–C1–Ge1 = 1.248(2); C2–C2–Ge1–C3 = 17.0(4).

comparable to the short Ge–C bonds in a germabenzene or germanaphthalene published by Tokitoh.^[21,22] This structural feature clearly underlines the double bond character in the germanium ylide. The closely related germenes $\text{Me}_2\text{Ge}=\text{CR}_2$ ^[23] (CR_2 =fluorenylidene) possess Ge–C distances of 1.803 and 1.806 Å. Only a slightly longer (1.827 Å) Ge–C distance was reported for a diboryl-stabilized germene.^[24] Thus, the germanium ylide **14** can clearly be regarded as a germene bearing a cationic phosphonium substituent.^[14a,25] The small C2–C1–Ge1–C3 dihedral angle of 17° support these findings. The Ge1–C3 bond length of 1.931(5) Å is in the expected range of Ge–C single bonds.^[26]

The double-bond character in the respective cationic silicon and germanium ylides **9**, **10**, and **14** is also corroborated by NBO and AIM analyses.^[27] For comparison, the silene $\text{Me}_2\text{C}=\text{SiMe}_2$ and silane $\text{Me}_3\text{C}-\text{SiMe}_3$ were investigated (Table 3). The three cationic ylides show typical characteristics of double bonds, with π -bond occupations between 1.82 and 1.85 e, bond ellipticities between 0.28 and 0.45, as well as Wiberg Bond Indices of greater than 1, between 1.25 and 1.30. Compared to properties of $\text{Me}_2\text{C}=\text{SiMe}_2$, all of these indicators are comparable but slightly smaller, which indicates less covalent character in the cationic double bonds. However, the bond polarization in the cationic ylides is considerably larger, with a negative charge between –1.12 and –1.20 e on C and a positive charge between +1.64 and +1.87 e on Si or Ge, respectively. These charges are larger than in the tetramethyl silene $\text{Me}_2\text{C}=\text{SiMe}_2$ (–0.62, +1.42 e). Therefore, the C–Si and C–Ge interactions in **9**, **10** and **14** can be interpreted as strongly polarized double bond systems. In accord with this interpretation, the depicted HOMO and LUMO of the converged structural model (TPSS/def2-TZVP) of **9** show the polarized orbital contributions (Figure 8).

Table 3. Bond analysis data on **9**, **10**, and **14** (NBO charges and orbital occupations in e, E = Si or Ge).

Comp.	Q (C)	Q (E)	Σ (C–E)	Π (C–E)	WBI	Ellipticity
$\text{Me}_2\text{CSiMe}_2$	–0.62	1.42	1.97	1.90	1.54	0.63
10	–1.20	1.82	1.96	1.85	1.30	0.45
9	–1.22	1.87	1.95	1.83	1.25	0.45
14	–1.12	1.64	1.94	1.82	1.26	0.28
$\text{Me}_3\text{CSiMe}_3$	–0.44	1.65	1.94	–	0.74	0.00

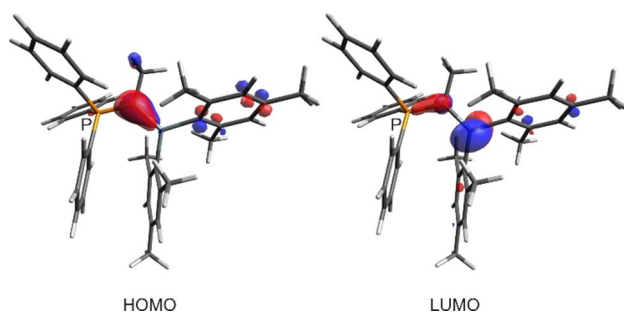


Figure 8. Calculated (TPSS/def2-TZVP) HOMO and LUMO (iso value = 0.07) of **9**.

Similar to the silicon derivative **9**, the FIA in the gas phase was calculated, furnishing a FIA of 624 kJ mol^{–1} ($\text{FIA}_{\text{solv}} = 522 \text{ kJ mol}^{-1}$) for **14**. The observed weakening of 66.5 kJ mol^{–1} compared to **9** can be attributed to the less electropositive character of Ge. Unfortunately, the Gutmann-Beckett-Method^[28] could not be applied due to dynamic processes in solution. Initial reactivity studies revealed that **14** shows no reactivity towards H₂, CO and CO₂, which might be a result of steric shielding.

Conclusion

In this work, the synthesis and full characterization of α -silylated (**1–7**) and α -germylated (**11–13**) phosphorus ylides of the general formula $\text{R}_3\text{PC}(\text{R}^1)\text{E}(\text{Cl})\text{R}^2$ is reported. The title compounds were fully characterized, including determination of their molecular structures by X-ray diffraction. We report the reactivity towards the abstraction of the chloride with sodium salts of the weakly coordination anions $\text{Na}[\text{B}(\text{C}_6\text{F}_5)_4]$ and $\text{Na}[\text{B}\{3,5-(\text{CF}_3)_2\text{C}_6\text{H}_3\}_4]$. The reaction of $\text{Ph}_3\text{PC}(\text{Me})\text{Si}(\text{Cl})\text{Me}_2$ (**1**) with $\text{Na}[\text{B}(\text{C}_6\text{F}_5)_4]$ furnished the dimeric phosphonium-like dication $[\text{Ph}_3\text{PC}(\text{Me})\text{SiMe}_2]_2[\text{B}(\text{C}_6\text{F}_5)_4]_2$ (**8**). To determine the organic auxiliary to prevent dimerization of the polarized C/Si π -bonds in the cationic α -Si+CPs, DFT calculations on 11 potential systems were performed. Mesityl- and *i*Pr-substituted derivatives were found to be suitable targets to access monomeric species. The highly reactive compounds $[\text{Ph}_3\text{PC}(\text{Me})\text{SiMe}_2][\text{B}(\text{C}_6\text{F}_5)_4]$ (**9**) and $[\text{Ph}_3\text{PC}(\text{Et})\text{SiPr}_2][\text{B}(\text{C}_6\text{F}_5)_4]$ (**10**) could be characterized by NMR spectroscopy and decompose in polar solvents. The less reactive germanium analogue $[\text{Ph}_3\text{PC}(\text{Me})\text{GeMe}_2][\text{B}\{3,5-(\text{CF}_3)_2\text{C}_6\text{H}_3\}_4]$ (**14**) was obtained by the reaction of **11** with $\text{Na}[\text{BAR}^f]$. Whereas **9** and **10** decompose rapidly in methylene chloride, **14** could be crystallized from this solvent and was fully characterized including X-ray diffraction analysis. Structural parameters in accord with NBO and AIM analyses provide clear evidence of a strong $\text{C}_{\text{ylide}}-\text{Ge}$ interaction with high double bond character. Studies in our lab continue to further explore the reactivity on neutral and cationic species of this type.

Experimental Section

General methods: All operations were carried out under dry argon using standard Schlenk and glovebox techniques. The phosphonium salts $\text{Ph}_3\text{PC}(\text{R})\text{H}_2\text{Br}$ were used as purchased from Sigma-Aldrich. The ylides $\text{Ph}_3\text{PC}(\text{R})\text{H}$ (R = Me, Et, Ph) were synthesized according to literature procedures,^[16] as well as Me_2GeCl_2 ,^[29] sodium salts $\text{Na}[\text{B}(\text{C}_6\text{F}_5)_4]$ ^[30] and $\text{Na}[\text{BAR}^f]$.^[31] Solvents were dried over Na/K and rigorously degassed before use. NMR spectra were recorded on Bruker AV 300 and 400 spectrometers in dry degassed deuterated solvents. ¹H, ¹³C{¹H} and ²⁹Si chemical shifts were reported against TMS and ³¹P{¹H} against H₃PO₄. Coupling constants (*J*) are given in Hertz as positive values, regardless of their real individual signs. The multiplicity of the signals is indicated as s, d, q, sept, or m for singlet, doublet, quartet, septet, or multiplet, respectively. The assignments were confirmed, as necessary, with the use of 2D NMR correlation experiments. IR spectra were measured on a Bruker Alpha spectrometer using the attenuated reflection technique (ATR) and the data are quoted in wave-

numbers [cm⁻¹]. The intensity of the absorption band is indicated as vw (very weak), w (weak), m (medium), s (strong), vs. (very strong), and br (broad). Melting points were measured with a Thermo Fischer melting point apparatus and are not corrected. Elemental analyses were carried out in the institutional technical laboratories of the Karlsruhe Institute of Technology (KIT). No satisfactory elemental analyses could be obtained for **11** and **12**, due to their sensitivity towards air and moisture, and for **8** and **14**, due to high fluorine content of the samples.

Computational details: For the calculations we used the ORCA 4.2 program.^[32] The DFT^[33] calculations were carried out with the functional TPSS^[34] and the basis set def2-TZVP.^[35] Calculations were done with the following settings of calculation parameters: grid size^[33b] 4, threshold for SCF energy change 10⁻⁶; convergence thresholds for the structure optimization: energy change 10⁻⁶ gradient norm 10⁻⁴. Natural bond orbital (NBO) analysis was performed with the NBO 6.0 program^[36] interfaced with Gaussian 09.^[37] The programs AIMAll^[38] and Multiwfn^[27] were used for QTAIM analysis.

Synthesis of 1–7: To a solution of 2 equiv. ylide Ph₃PC(R)H (R = Me, Et, Ph) in toluene 1 equiv. of the appropriate dichlorosilane R₂SiCl₂ (R = Me, Et, *i*Pr, Mes) was added at room temperature. The reaction mixture was heated for hours to days (Table 4). After filtration and evaporation of the solvent the crude product was recrystallized from hot hexane to afford 1–7 as yellow crystalline solids in yields of 30–83% (Table 4).

1: M.p. (decomp.): 115 °C. ¹H NMR (300 MHz, 298 K, C₆D₆): δ = 7.74–7.66 (m, H_{Ph_ortho} 6H), 7.10–7.00 (m, H_{Ph_meta+para} 9H), 1.97 (d, ³J_{PH} = 19.7 Hz, H_{YlideMer} 3H), 0.33 ppm (s, H_{SiMe} 6H). ¹³C{¹H} NMR (75 MHz, 298 K, C₆D₆): δ = 134.3 (d, ²J_{PC} = 9.4 Hz, C_{Ph_ortho}), 131.4 (d, ⁴J_{PC} = 2.7 Hz, C_{Ph_para}), 130.9 (d, ¹J_{PC} = 84.6 Hz, C_{Ph_ippo}), 128.5 (d, ³J_{PC} = 10.9 Hz, C_{Ph_meta}), 14.9 (d, ²J_{PC} = 1.3 Hz, C_{YlideMe}), 7.8 (d, ¹J_{PC} = 97.6 Hz, C_{YlideC}), 5.1 ppm (d, ³J_{PC} = 3.2 Hz, C_{SiMe}). ³¹P{¹H} NMR (121 MHz, 298 K, C₆D₆): δ = 22.5 ppm (s). ²⁹Si NMR (60 MHz, 298 K, C₆D₆): δ = 21.3 ppm (d, ²J_{PSi} = 31.1 Hz). IR (ATR, cm⁻¹): ν̄ = 3055 (vw), 2962 (vw), 2907 (vw), 2840 (vw), 1587 (vw), 1479 (vw), 1434 (m), 1403 (vw), 1309 (vw), 1246 (m), 1149 (m), 1098 (s), 1026 (vw), 997 (w), 923 (s), 861 (vw), 837 (m), 804 (m), 777 (s), 747 (s), 691 (vs), 670 (s), 585 (s), 530 (s), 508 (vs), 475 (s), 418 (s), 383 (w). Elemental analysis (%): C₂₂H₂₄ClPSi calcd. C 69.00, H 6.32; meas. C 72.12, H 6.02.

2: M.p.: 110 °C. ¹H NMR (300 MHz, 298 K, C₆D₆): δ = 7.77–7.70 (m, H_{Ph_ortho} 6H), 7.10–7.01 (m, H_{Ph_meta+para} 9H), 1.96 (d, ³J_{PH} = 19.6 Hz, H_{YlideMer} 3H), 1.12 (t, ³J_{HH} = 7.9 Hz H_{SiCH₂CH₃}, 6H), 1.12 ppm (ds, ³J_{HH} = 7.9 Hz H_{SiCH₂CH₃}, 4H). ¹³C{¹H} NMR (75 MHz, 298 K, C₆D₆): δ = 134.0 (d, ²J_{PC} = 8.9 Hz, C_{Ph_ortho}), 131.1 (d, ⁴J_{PC} = 2.8 Hz, C_{Ph_para}), 130.6 (d, ¹J_{PC} = 84.0 Hz, C_{Ph_ippo}), 128.2 (d, ³J_{PC} = 11.1 Hz, C_{Ph_meta}), 14.7 (d, ²J_{PC} = 1.28 Hz, C_{YlideMe}), 9.6 (d, ³J_{PC} = 3.3 Hz, C_{SiCH₂CH₃}), 9.6 (s, C_{SiCH₂CH₃}), 4.1 ppm (d, ¹J_{PC} = 97.6 Hz, C_{YlideC}). ³¹P{¹H} NMR (121 MHz, 298 K, C₆D₆): δ = 22.7 ppm (s). ²⁹Si NMR (60 MHz, 298 K, C₆D₆): δ = 27.5 ppm (d, ²J_{PSi} = 28.9 Hz). IR (ATR, cm⁻¹): ν̄ = 2962 (vw), 2911 (vw), 2876 (vw), 1587 (vw), 1480 (vw), 1433 (m), 1311 (vw), 1238 (vw), 1170 (w), 1109 (m), 1090 (m), 1061 (w), 1001 (w), 927 (m), 751 (s),

729 (s), 689 (vs), 673 (s), 642 (w), 582 (m), 530 (vs), 506 (vs), 488 (s), 464 (w), 438 (m), 427 (m), 382 (w). Elemental analysis (%): C₂₄H₂₈ClPSi calcd. C 70.14, H 6.87; meas. C 72.49, H 6.59.

3: M.p. (decomp.): 194 °C. ¹H NMR (300 MHz, 298 K, C₆D₆): δ = 7.67–7.60 (m, H_{Ph_ortho} 6H), 7.06–6.90 (m, H_{Ph_meta+para} 12H), 6.56 (brs, H_{Mes_meta}), 2.61 (brs, H_{Mes_orthoMer} 12H), 2.17 (d, ³J_{PH} = 19.5 Hz, H_{YlideMer} 3H), 2.06 ppm (s, H_{Mes_paraMer} 6H). ¹³C{¹H} NMR (75 MHz, 298 K, C₆D₆): δ = 144.5 (brs, C_{Ortho-Mes}), 137.9 (s, C_{para-Mes}), 136.0 (brs, C_{ippo-Mes}), 134.1 (d, ²J_{PC} = 9.2 Hz, C_{ortho-Ph}), 130.9 (d, ⁴J_{PC} = 2.7 Hz, C_{para-Ph}), 129.9 (s, C_{meta-Mes}), 128.2 (d, ³J_{PC} = 11.4 Hz, C_{meta-Ph}), 24.7 (brs, C_{ortho-Me}), 21.0 ppm (s, C_{para-Me}), 18.3 (s, C_{PCCH₃}). ³¹P{¹H} NMR (121 MHz, 298 K, C₆D₆): δ = 23.2 ppm (s). ²⁹Si NMR (60 MHz, 298 K, C₆D₆): δ = 0.54 ppm (d, ²J_{PSi} = 37.1 Hz). IR (ATR, cm⁻¹): ν̄ = 2916 (vw), 1603 (w), 1434 (m), 1405 (w), 1375 (m), 1304 (m), 1232 (m), 1160 (s), 1095 (w), 1041 (m), 924 (vs), 868 (w), 845 (m), 822 (vw), 752 (w), 744 (m), 706 (s), 695 (vs), 637 (s), 621 (s), 587 (w), 552 (m), 530 (s), 511 (vs), 488 (w), 454 (vs), 432 (s), 398 (s). Elemental analysis (%): C₃₈H₄₀ClPSi calcd. C 77.20, H 6.82; meas. C 76.11, H 6.78.

4: M.p. (decomp.): 130 °C. ¹H NMR (300 MHz, 298 K, C₆D₆): δ = 7.75–7.70 (m, H_{Ph_ortho} 6H), 7.09–7.01 (m, H_{Ph_meta+para} 9H), 2.35 (m, H_{YlideCH₂CH₃}, 2H), 1.12 (t, ³J_{HH} = 7.2 Hz H_{YlideCH₂CH₃}, 3H), 0.37 ppm (s, H_{SiMe} 6H). ¹³C{¹H} NMR (75 MHz, 298 K, C₆D₆): δ = 134.3 (d, ²J_{PC} = 9.2 Hz, C_{Ph_ortho}), 131.6 (d, ¹J_{PC} = 83.7 Hz, C_{Ph_ippo}), 131.4 (d, ⁴J_{PC} = 2.8 Hz, C_{Ph_para}), 128.2 (d, ³J_{PC} = 11.1 Hz, C_{Ph_meta}), 22.8 (d, ²J_{PC} = 2.4 Hz, C_{YlideCH₂CH₃}), 20.8 (d, ³J_{PC} = 2.0 Hz, C_{YlideCH₂CH₃}), 17.7 (d, ¹J_{PC} = 94.1 Hz, C_{YlideC}), 5.48 ppm (d, ³J_{PC} = 3.1 Hz, C_{SiMe}). ³¹P{¹H} NMR (121 MHz, 298 K, C₆D₆): δ = 23.7 ppm (s). ²⁹Si NMR (60 MHz, 298 K, C₆D₆): δ = 20.2 ppm (d, ²J_{PSi} = 32.7 Hz). IR (ATR, cm⁻¹): ν̄ = 3072 (vw), 2962 (vw), 2886 (vw), 2793 (vw), 1588 (vw), 1480 (vw), 1456 (vw), 1435 (m), 1404 (vw), 1363 (vw), 1310 (vw), 1256 (w), 1245 (w), 1144 (w), 1099 (s), 1028 (vw), 998 (w), 978 (m), 925 (m), 860 (vw), 837 (w), 805 (m), 769 (m), 746 (s), 694 (vs), 670 (m), 580 (m), 530 (vs), 514 (vs), 485 (s), 467 (m), 417 (s). Elemental analysis (%): C₂₃H₂₆ClPSi calcd. C 69.59, H 6.60; meas. C 68.77, H 6.13.

5: M.p.: 110 °C. ¹H NMR (300 MHz, 298 K, C₆D₆): δ = 7.80–7.75 (m, H_{Ph_ortho} 6H), 7.07–7.03 (m, H_{Ph_meta+para} 9H), 2.35 (m, H_{YlideCH₂CH₃}, 2H), 1.12 (m, H_{YlideCH₂CH₃}, overlaid with H_{SiCH₂CH₃}, 9H), 0.71 ppm (m, H_{SiCH₂CH₃}, 4H). ¹³C{¹H} NMR (75 MHz, 298 K, C₆D₆): δ = 134.0 (d, ²J_{PC} = 9.6 Hz, C_{Ph_ortho}), 131.6 (d, ¹J_{PC} = 83.4 Hz, C_{Ph_ippo}), 131.4 (d, ⁴J_{PC} = 2.8 Hz, C_{Ph_para}), 128.2 (d, overlaid with C₆D₆, C_{Ph_meta}), 22.4 (d, ²J_{PC} = 2.5 Hz, C_{YlideCH₂CH₃}), 20.4 (d, ³J_{PC} = 2.0 Hz, C_{YlideCH₂CH₃}), 14.7 (d, ¹J_{PC} = 93.9 Hz, C_{YlideC}), 10.0 (d, ³J_{PC} = 3.1 Hz, C_{SiCH₂CH₃}), 8.2 ppm (s, C_{SiCH₂CH₃}). ³¹P{¹H} NMR (121 MHz, 298 K, C₆D₆): δ = 23.5 ppm (s). ²⁹Si NMR (60 MHz, 298 K, C₆D₆): δ = 26.5 ppm (d, ²J_{PSi} = 30.5 Hz). IR (ATR, cm⁻¹): ν̄ = 3074 (vw), 3052 (vw), 2955 (w), 2925 (vw), 2872 (vw), 1587 (vw), 1480 (vw), 1457 (vw), 1434 (m), 1360 (vw), 1311 (vw), 1280 (vw), 1236 (vw), 1179 (vw), 1137 (m), 1097 (s), 1028 (vw), 998 (w), 970 (s), 918 (m), 858 (vw), 752 (s), 708 (vs), 692 (vs), 668 (s), 640 (m), 574 (m), 529 (s), 516 (vs), 486 (s), 466 (m), 435 (s). Elemental analysis (%): C₂₅H₃₀ClPSi calcd. C 70.65, H 7.11; meas. C 72.03, H 6.63.

6: M.p.: 100 °C. ¹H NMR (300 MHz, 298 K, C₆D₆): δ = 7.85–7.78 (m, H_{Ph_ortho} 6H), 7.07–7.03 (m, H_{Ph_meta+para} 9H), 2.39 (m, H_{YlideCH₂CH₃}, 2H), 1.27 (d, ³J_{HH} = 2.7 Hz, H_{YlideCH₂CH₃}, 3H), 1.24 (d, ³J_{HH} = 2.7 Hz, H_{SiCH₂CH₃}, 6H), 0.87 ppm (sept, ³J_{HH} = 7.41 Hz H_{SiCH₂CH₃}, 2H). ¹³C{¹H} NMR (75 MHz, 298 K, C₆D₆): δ = 134.7 (d, ²J_{PC} = 9.2 Hz, C_{Ph_ortho}), 131.3 (d, ¹J_{PC} = 84.2 Hz, C_{Ph_ippo}), 131.4 (d, ⁴J_{PC} = 4.9 Hz, C_{Ph_para}), 128.0 (d, ³J_{PC} = 11.3 Hz, C_{meta-Ph}), 23.3 (d, ²J_{PC} = 2.0 Hz, C_{YlideCH₂CH₃}), 20.5 (d, ³J_{PC} = 1.7 Hz, C_{YlideCH₂CH₃}), 19.7 (s, C_{SiCH₂CH₃}), 19.3 (s, C_{SiCH₂CH₃}), 17.6 (d, ³J_{PC} = 3.1 Hz, C_{SiCH₂CH₃}), 12.5 ppm (d, ¹J_{PC} = 93.1 Hz, C_{YlideC}). ³¹P{¹H} NMR (121 MHz, 298 K, C₆D₆): δ = 22.9 ppm (s). ²⁹Si NMR (60 MHz, 298 K, C₆D₆): δ = 28.8 ppm (bs). IR (ATR, cm⁻¹): ν̄ = 3072 (vw), 3051 (vw), 2968 (vw), 2951 (vw), 2923 (vw), 2862 (w), 2212 (vw), 2163 (vw), 1587 (vw), 1574 (vw), 1481 (vw), 1462 (vw), 1434 (m), 1382 (vw),

Table 4. Reaction conditions and yields for the syntheses of 1–7. With R¹ at the α-carbon atom and R² at the silicon atom.

Comp.	R on C _{Ylide} (R ¹)	R on E (R ²)	T [°C]	t [h]	Yield [%]
1	Me	Me	95	96	59
2	Me	Et	110	48	52
3	Me	Mes	90	120	48
4	Et	Me	85	24	30
5	Et	Et	70	18	83
6	Et	<i>i</i> Pr	70	48	43
7	Ph	Me	60	48	49

1362 (vw), 1305 (vw), 1268 (vw), 1242 (vw), 1181 (vw), 1137 (m), 1093 (m), 1070 (m), 1028 (vw), 996 (w), 966 (m), 909 (w), 879 (w), 857 (vw), 845 (vw), 752 (s), 695 (vs), 671 (m), 647 (m), 626 (vw), 578 (m), 532 (s), 516 (s). Elemental analysis (%): C₂₇H₃₃ClPSi calcd. C 71.58, H 7.56; meas. C 72.70, H 7.08.

7: M.p.: 119 °C. ¹H NMR (300 MHz, 298 K, C₆D₆): δ = 7.78–7.67 (m, H_{PPh₃_ortho} 6H), 7.48–7.45 (m, H_{YlidePh_ortho} 2H), 7.03–6.98 (m, H_{PPh₃_meta+para} 9H), 6.88–6.84 (m, H_{YlidePh_meta+para} 3H), 0.34 ppm (s, H_{SiMe₂} 6H). ¹³C{¹H} NMR (75 MHz, 298 K, C₆D₆): δ = 144.0 (s, C_{Ph_para}) 134.3 (d, ²J_{PC} = 9.3 Hz, C_{PPh₃_ortho}), 134.2 (d, ³J_{PC} = 8.5 Hz, C_{Ph_ortho}) 131.5 (d, ⁴J_{PC} = 3.1 Hz, C_{PPh₃_para}), 131.5 (d, ²J_{PC} = 3.1 Hz, C_{Ph_ipso}), 130.9 (d, ¹J_{PC} = 85.3 Hz, C_{PPh₃_ipso}), 128.5 (d, ³J_{PC} = 11.5 Hz, C_{PPh₃_meta}), 123.2 (d, ⁴J_{PC} = 2.6 Hz, C_{Ph_meta}), 27.7 (d, ¹J_{PC} = 98.1 Hz, C_{YlideC}), 5.9 ppm (d, ³J_{PC} = 2.5 Hz, C_{SiMe}). ³¹P{¹H} NMR (121 MHz, 298 K, C₆D₆): δ = 17.2 ppm (s). ²⁹Si NMR (60 MHz, 298 K, C₆D₆): δ = 16.1 ppm (d, ²J_{PSi} = 28.5 Hz). IR (ATR, cm⁻¹): ν̄ = 3075 (vw), 2959 (vw), 2199 (vw), 2181 (vw), 1964 (vw), 1587 (w), 1481 (w), 1434 (m), 1400 (vw), 1308 (vw), 1251 (w), 1212 (m), 1183 (vw), 1157 (vw), 1096 (m), 1060 (w), 1035 (w), 1020 (m), 995 (w), 903 (m), 877 (vw), 837 (w), 825 (w), 805 (m), 775 (w), 747 (s), 711 (m), 688 (vs), 629 (w), 583 (vw), 520 (s), 498 (vs), 471 (m), 452 (m), 438 (s), 421 (m). Elemental analysis (%): C₂₇H₂₆ClPSi calcd. C 72.87, H 8.89; meas. C 75.38, H 5.48.

Synthesis of 6dec: In a glovebox, a vial was charged with **6** (100 mg, 0.22 mmol), Na[B(C₆F₅)₄] (155 mg, 0.22 mmol) and *i*Pr₂O (5 mL). After stirring overnight, the light-yellow suspension was filtered and layered with hexane (10 mL). After 5 days, the supernatant was removed and the remaining sticky solid was washed with 5 mL toluene. Drying under high vacuum yielded (30 mg, 12%) pure **6dec** as colorless sticky solid. Crystals suitable for XRD were obtained by layering a solution of **6dec** in *i*Pr₂O with hexane.

Synthesis of 8: A Schlenk tube was charged with **3** (260 mg, 0.68 mmol) and Na[B(C₆F₅)₄] (477 mg, 0.68 mmol) and toluene (18 mL). After stirring overnight, the resulting colorless suspension was filtered and the remaining solid was extracted with CH₂Cl₂ (10 mL). After a second filtration and concentration the solution was stored at 4 °C for 3 days. Removing the supernatant and drying under high vacuum yielded **8** (98 mg, 14 mmol, 21%) as colorless crystals (*cis:trans* = 0.6:1). Crystals suitable for XRD were obtained by slow concentration of a CH₂Cl₂ solution of **8**. **Trans isomer:** ¹H NMR (300 MHz, 298 K, CD₂Cl₂): δ = 7.92–7.82 (m, H_{Ph_para} 12H), 7.74–7.62 (m, H_{Ph_ortho} 24H), 7.47–7.30 (m, H_{Ph_meta} 24H), 1.56 (d, ³J_{PH} = 20.7 Hz, H_{YlideMer} 6H). 0.32 ppm (s, H_{SiMe}, 12H). ¹³C{¹H} NMR (75 MHz, 298 K, CD₂Cl₂): δ = 136.6 (s, C_{Ph_ortho}), 134.1 (brs, C_{Ph_para} overlap with *trans* isomer), 131.6 (m, C_{Ph_meta} overlap with *trans* isomer), 21.9 (s, C_{YlideMe}), 2.2 ppm (s, C_{SiMe}). ³¹P{¹H} NMR (121 MHz, 298 K, CD₂Cl₂): δ = 35.5 ppm (s). ²⁹Si NMR (60 MHz, 298 K, CD₂Cl₂): δ = 24.3 ppm (t, ²J_{PSi} = 4.1 Hz). **Cis isomer:** ¹H NMR (300 MHz, 298 K, CD₂Cl₂): δ = 7.92–7.82 (m, H_{Ph_para} 12H), 7.74–7.62 (m, H_{Ph_ortho} 24H), 7.47–7.30 (m, H_{Ph_meta} 24H), 1.85 (d, ³J_{PH} = 20.6 Hz, H_{YlideMer} 6H). 0.93 (s, H_{SiMe}, 6H), –0.05 ppm (s, H_{SiMe}, 6H). ¹³C{¹H} NMR (75 MHz, 298 K, CD₂Cl₂): δ = 136.5 (s, C_{Ph_ortho}), 134.1 (brs, C_{Ph_para} overlap with *trans* isomer), 131.6 (m, C_{Ph_meta} overlap with *trans* isomer), 23.7 (s, C_{YlideMe}), 3.9 (s, C_{SiMe}), –0.4 ppm (d, C_{SiMe}). ³¹P{¹H} NMR (121 MHz, 298 K, CD₂Cl₂): δ = 36.3 ppm (s). ²⁹Si NMR (60 MHz, 298 K, CD₂Cl₂): δ = 22.6 ppm (t, ²J_{PSi} = 3.8 Hz). ¹¹B NMR (96 MHz, 298 K, CD₂Cl₂): δ = –16.7 ppm (s). ¹⁹F NMR (282 MHz, 298 K, CD₂Cl₂): δ = –133.0 (m, B(C₆F₅)₄_meta), –163.5 (t, ²J_{FF} = 20.4 Hz B(C₆F₅)₄_ortho), –167.4 ppm (t, ²J_{FF} = 19.0 Hz B(C₆F₅)₄_para). IR (ATR, cm⁻¹): ν̄ = 1643 (vw), 1588 (vw), 1513 (m), 1461 (vs), 1438 (s), 1375 (vw), 1273 (w), 1212 (vw), 1084 (vs), 1020 (vw), 977 (vs), 942 (w), 906 (w), 831 (s), 803 (w), 774 (m), 746 (s), 733 (m), 712 (w), 689 (vs), 660 (s), 612 (w), 574 (vw), 553 (m), 524 (s), 505 (m), 471 (w), 435 (w), 397 (w), 382 (vw). Elemental analysis: Due to the high fluorine content, no appropriate elemental analysis was obtained. *Due to poor solubility, the multiplets could not be

resolved and no signal for the ipso-C and ylide-C as well as for the [B(C₆F₅)₄] anion could be detected.

Synthesis of 11: To a solution of ylide Ph₃PC(Me)H (1.60 g, 4.96 mmol) in toluene Me₂GeCl₂ (0.50 g, 0.34 mL, 2.84 mmol) was added at room temperature. After stirring for 15 min at room temperature, filtration and evaporation of the solvent the crude product was recrystallized from hot hexane and the supernatant layer was removed. Drying in high vacuum yielded pure **11** (121 mg, 10%) as light-yellow crystals suitable for XRD. M.p.: 141 °C. ¹H NMR (300 MHz, 298 K, C₆D₆): δ = 7.75–7.68 (m, H_{Ph_ortho} 6H), 7.06–7.03 (m, H_{Ph_meta+para} 9H), 2.08 (d, ³J_{PH} = 18.9 Hz, H_{YlideMer} 3H), 0.47 ppm (s, H_{GeMe}, 6H). ¹³C{¹H} NMR (75 MHz, 298 K, C₆D₆): δ = 134.3 (d, ²J_{PC} = 9.2 Hz, C_{Ph_ortho}), 131.5 (d, ⁴J_{PC} = 2.8 Hz, C_{Ph_para}), 130.8 (d, ¹J_{PC} = 84.7 Hz, C_{Ph_ipso}), 128.6 (d, ³J_{PC} = 10.9 Hz, C_{Ph_meta}), 15.4 (d, ¹J_{PC} = 98.2 Hz, C_{YlideC}), 15.3 (d, ²J_{PC} = 2.9 Hz, C_{YlideMe}), 6.2 ppm (d, ³J_{PC} = 4.0 Hz, C_{GeMe}). ³¹P{¹H} NMR (121 MHz, 298 K, C₆D₆): δ = 21.8 ppm (s). IR (ATR, cm⁻¹): ν̄ = 3050 (vw), 2988 (vw), 2909 (vw), 2838 (vw), 1587 (vw), 1484 (vw), 1433 (s), 1375 (vw), 1310 (vw), 1237 (vw), 1144 (w), 1114 (w), 1100 (s), 1071 (w), 1026 (vw), 997 (w), 894 (m), 861 (w), 833 (w), 806 (w), 775 (vw), 749 (s), 735 (w), 708 (m), 691 (vs), 611 (m), 598 (m), 564 (m), 527 (s), 506 (vs), 459 (m), 435 (w).

Synthesis of 12: To a solution of ylide Ph₃PC(Ph)H (2.00 g, 4.96 mmol) in toluene Me₂GeCl₂ (0.50 g, 0.34 mL, 2.84 mmol) was added at room temperature. After heating to 90 °C for 15 min, filtration, concentration of the solution and cooling to –40 °C for four weeks, the supernatant layer was removed. Drying in high vacuum yielded pure **12** (457 mg, 33%) as light-yellow crystals suitable for XRD. M.p.: 115 °C. ¹H NMR (300 MHz, 298 K, C₆D₆): δ = 7.78–7.70 (m, H_{PPh₃_ortho} 6H), 7.49–7.46 (m, H_{YlidePh_ortho} 2H), 7.03–6.98 (m, H_{PPh₃_meta+para} 9H), 6.86–6.81 (m, H_{YlidePh_meta+para} 3H), 0.48 ppm (s, H_{GeMer} 6H). ¹³C{¹H} NMR (75 MHz, 298 K, C₆D₆): δ = 144.5 (d, ⁵J_{CP} = 3.1 Hz C_{Ph_para}) 134.4 (d, ²J_{PC} = 10.1 Hz, C_{PPh₃_ortho}), 132.3 (d, ³J_{PC} = 9.7 Hz, C_{Ph_ortho}) 131.7 (d, ⁴J_{PC} = 3.5 Hz, C_{PPh₃_para}), 130.6 (d, ¹J_{PC} = 85.8 Hz, C_{PPh₃_ipso}), 128.6 (d, ³J_{PC} = 11.5 Hz, C_{PPh₃_meta}), 122.5 (d, ⁴J_{PC} = 1.9 Hz, C_{Ph_meta}), 33.28 (d, ¹J_{PC} = 102.3 Hz, C_{YlideC}), 7.4 ppm (d, ³J_{PC} = 2.9 Hz, C_{GeMe}). ³¹P{¹H} NMR (121 MHz, 298 K, C₆D₆): δ = 15.6 ppm (s). IR (ATR, cm⁻¹): ν̄ = 3073 (vw), 2202 (vw), 2185 (vw), 2167 (vw), 2032 (vw), 1587 (w), 1560 (vw), 1480 (w), 1433 (m), 1407 (vw), 1309 (vw), 1221 (m), 1182 (w), 1157 (vw), 1089 (m), 1038 (vw), 996 (m), 881 (m), 871 (w), 841 (w), 822 (w), 806 (m), 748 (s), 711 (m), 688 (vs), 637 (w), 604 (w), 583 (w), 523 (vs), 498 (vs), 470 (m), 443 (w), 428 (w), 411 (w), 394 (vw).

Synthesis of 13: Mes₂GeCl₂ (1.00 g, 2.62 mmol) and Ph₃PC(Me)H (1.52 g, 5.24 mmol) were dissolved in 10 mL toluene. After heating the mixture for 2 h to 90 °C, a colorless precipitate was formed and the color changed from orange to yellow. After filtration, evaporation of the solvent and recrystallization from a small amount of toluene the supernatant layer was removed. Drying in high vacuum yielded pure **13** (812 mg, 49%) as yellow crystalline solid. Crystals suitable for XRD were obtained from saturated toluene solution of **13**. M.p. (decomp.): 236 °C. ¹H NMR (300 MHz, 298 K, C₆D₆): δ = 7.71–7.64 (m, H_{Ph_ortho} 6H), 7.00–6.89 (m, H_{Ph_meta+para} 9H), 6.53 (brs, H_{MesChr} 4H), 2.62 (brs, H_{Mes_ortho-Mer} 12H), 2.34 (d, ³J_{PH} = 18.8 Hz, H_{YlideMer} 3H), 2.04 ppm (s, H_{Mes_para-Mer} 6H). ¹³C{¹H} NMR (75 MHz, 298 K, C₆D₆): δ = 143.3 (bs, C_{Mes_ortho}), 139.0 (d, ³J_{PC} = 4.3 Hz, C_{Mes_ipso}), 137.8 (s, C_{Mes_para}), 134.1 (d, ²J_{PC} = 9.3 Hz, C_{Ph_ortho}), 131.1 (d, ⁴J_{PC} = 2.8 Hz, C_{Ph_para}), 130.4 (d, ¹J_{PC} = 97.8 Hz, C_{Ph_ipso}), 129.7 (s, C_{Mes_meta}), 128.2 (d, ³J_{PC} = 11.4 Hz, C_{Ph_meta}), 24.1 (brs, C_{Mes_ortho-Me}), 20.9 (s, C_{Mes_para-Me}), 18.4 (d, ²J_{PC} = 2.9 Hz, C_{YlideMe}), 15.9 ppm (d, ²J_{PC} = 9.3 Hz, C_{YlideC}). ³¹P{¹H} NMR (121 MHz, 298 K, C₆D₆): δ = 21.8 ppm (s). IR (ATR, cm⁻¹): ν̄ = 3054 (vw), 2915 (vw), 2851 (vw), 2170 (vw), 1972 (vw), 1602 (vw), 1553 (vw), 1481 (vw), 1436 (m), 1405 (vw), 1379 (vw), 1311 (vw), 1286 (vw), 1185 (vw), 1150 (m), 1104 (w), 1091 (w), 1050 (w), 1028 (vw), 997 (vw), 907 (vs), 844 (m), 751 (m), 744 (m), 706 (vs), 695 (vs), 588 (m), 576 (s), 549 (w), 522 (vs), 506 (vs), 480 (vw), 457 (vw), 425 (vw),

404 (vw), 386 (vw). Elemental analysis (%): C₃₈H₄₀ClGeP calcd. C 71.79, H 6.34; meas. C 71.49, H 5.99.

Synthesis of 14: To a solution of **13** (300 mg, 0.47 mmol) in toluene (10 mL) Na[B(3,5-(CF₃)₂C₆H₃)₄] (418 mg, 0.47 mmol) was added. After short stirring, two phases formed. Removing the solvent in vacuo and storing the resulting oil at -40 °C over night again two phases formed. The remaining toluene was quickly evaporated. CH₂Cl₂ (1 mL) and pentane (5 mL) were added to the oily residue. The solvent was removed by syringe and the remaining solid was dried in high vacuum. Recrystallization from CH₂Cl₂ by slow concentration of the solution yielded **14** (200 mg, 30%) in pure form as light-yellow crystals suitable for XRD. M.p.: 158 °C. ¹H NMR (300 MHz, 298 K, C₆D₆): δ = 8.41 (s, H_{BAr^F_ortho}, 8H), 7.64 (s, H_{BAr^F_para}, 4H), 7.21–7.14 (m, H_{A_ortho}, 6H), 6.99–6.93 (m, H_{A_para}, 3H), 6.90–6.82 (m, H_{A_meta}, 6H), 6.64 (s, H_{Mes2r}, 2H), 6.15 (s, H_{Mes1r}, 2H), 2.12 (s, H_{Mes2_orthoMer}, 6H), 2.03 (s, H_{Mes2_paraMe}), 1.87 (s, H_{Mes1_paraMe}), 1.78 (s, H_{Mes1_orthoMer}, 6H), 1.77 ppm (d, ³J_{PH} = 18.2 Hz, H_{YlideMer}, 3H). ¹³C{¹H} NMR (75 MHz, 298 K, C₆D₆ and PhF): δ = 162.8 (q, ¹J_{BC} = 49.7 Hz, C_{ipso-BAr^F}), 143.0 (s, C_{para-Mes2}), 142.2 (s, C_{ortho-Mes2}), 142.1 (s, C_{para-Mes1}), 140.5 (s, C_{ortho-Mes1}), 135.5 (brs, C_{ortho-BAr^F}), 134.2 (d, ⁴J_{PC} = 2.8 Hz, C_{para-Ph}), 133.5 (d, ²J_{PC} = 9.7 Hz, C_{ortho-Ph}), 129.6 (s, C_{meta-Mes2}), 129.6 (d, ³J_{PC} = 12.2 Hz, C_{meta-Ph}), 128.9 (s, C_{meta-Mes1}), 125.3 (q, ¹J_{CF} = 273 Hz, C_{CF3}), 120.9 (d, ¹J_{PC} = 67.0 Hz, C_{ipso-Ph}), 118.0 (brs, C_{para-BAr^F}), 24.6 (s, C_{ortho-Me-Mes1}), 23.4 (s, C_{ortho-Me-Mes2}), 20.9 (s, C_{para-Me-Mes1}), 20.6 (s, C_{ortho-Me-Mes2}), 17.6 (s, C_{YlideMe}). In addition, with HMBC determined: 134.7 (s, C_{ipso-M2}), 131.0 (s, C_{ipso-Mes2}), 90.5 (d, ¹J_{PC} = 80 Hz, C_{Ylide}). The resonance for meta-C of BA^rF could not be detected due to overlay with PhF. ¹¹B NMR (96 MHz, 298 K, C₆D₆): δ = -5.9 ppm (s) ¹⁹F NMR (282 MHz, 298 K, C₆D₆): δ = -62.26 ppm (s). ³¹P{¹H} NMR (121 MHz, 298 K, C₆D₆): δ = 24.6 ppm (s). IR (ATR, cm⁻¹): $\tilde{\nu}$ = 1607 (vw), 1439 (vw), 1352 (s), 1275 (vs), 1161 (m), 1118 (vs), 1104 (vs), 1028 (vw), 999 (vw), 929 (vw), 885 (m), 854 (vw), 838 (w), 744 (w), 713 (m), 693 (w), 681 (m), 668 (m), 595 (vw), 575 (w), 566 (vw), 547 (vw), 515 (m), 447 (vw), 382 (vw). Elemental analysis: due to the high fluorine content no appropriate elemental analysis was obtained.

Crystallographic details: Deposition Numbers (2098527 (for **1**), 2098528 (for **2**), 2098529 (for **3**), 2098530 (for **4**), 2098531 (for **5**), 2098532 (for **6**), 2098533 (for **6dec**), 2098534 (for **7**), 2098535 (for **8**), 2098536 (for **11**), 2098537 (for **12**), 2098538 (for **13**), 2098539 (for **14**), 2098540 (for Mes₂GeCl₂)) contain the supplementary crystallographic data for this paper. These data are provided free of charge by the joint Cambridge Crystallographic Data Centre and Fachinformationszentrum Karlsruhe Access Structures service.

Acknowledgements

We acknowledge Bernhard Birenheide and Dr. Hanna Wagner for their great help with the X-ray crystal structures. Open Access funding enabled and organized by Projekt DEAL.

Conflict of Interest

The authors declare no conflict of interest.

Data Availability Statement

The data that support the findings of this study are available in the supplementary material of this article.

Keywords: ambiphilic molecules · electronic frustration · geryllium cations · silylium cations · ylides

- [1] a) D. W. Stephan, G. Erker, *Angew. Chem. Int. Ed.* **2010**, *49*, 46–76; *Angew. Chem.* **2010**, *122*, 50–81; b) D. W. Stephan, *J. Am. Chem. Soc.* **2015**, *137*, 10018–10032; c) D. W. Stephan, *Acc. Chem. Res.* **2015**, *48*, 306–316; d) D. W. Stephan, G. Erker, *Angew. Chem. Int. Ed.* **2015**, *54*, 6400–6441; *Angew. Chem.* **2015**, *127*, 6498–6541; e) D. W. Stephan, *Science* **2016**, *354*, aaf7229; f) G. C. Welch, R. R. S. Juan, J. D. Masuda, D. W. Stephan, *Science* **2006**, *314*, 1124–1126.
- [2] a) A. Schäfer, M. Reißmann, A. Schäfer, W. Saak, D. Haase, T. Müller, *Angew. Chem. Int. Ed.* **2011**, *50*, 12636–12638; *Angew. Chem.* **2011**, *123*, 12845–12848; b) M. Reißmann, A. Schäfer, S. Jung, T. Müller, *Organometallics* **2013**, *32*, 6736–6744; c) T. J. Herrington, B. J. Ward, L. R. Doyle, J. McDermott, A. J. P. White, P. A. Hunt, A. E. Ashley, *Chem. Commun.* **2014**, *50*, 12753–12756; d) J. Li, Y. Li, I. Purushothaman, S. De, B. Li, H. Zhu, P. Parameswaran, Q. Ye, W. Liu, *Organometallics* **2015**, *34*, 4209–4217; e) N. von Wolff, G. Lefèvre, J. C. Berthet, P. Thuéry, T. Cantat, *ACS Catal.* **2016**, *6*, 4526–4535; f) A. Adenot, N. von Wolff, G. Lefèvre, J.-C. Berthet, P. Thuéry, T. Cantat, *Chem. Eur. J.* **2019**, *25*, 8118–8126; g) A. Dajnak, E. Maerten, N. Saffon-Merceron, A. Baceiredo, T. Kato, *Organometallics* **2020**, *39*, 3403–3412.
- [3] a) S. Schwendemann, S. Oishi, S. Saito, R. Fröhlich, G. Kehr, G. Erker, *Chem. Asian J.* **2013**, *8*, 212–217; b) S. Styra, M. Radius, E. Moos, A. Bihlmeier, F. Breher, *Chem. Eur. J.* **2016**, *22*, 9508–9512; c) M. Simon, M. Radius, H. E. Wagner, F. Breher, *Eur. J. Inorg. Chem.* **2020**, 1906–1914; d) S. Roters, C. Appelt, H. Westenberger, A. Hepp, J. C. Slootweg, K. Lammertsma, W. Uhl, *Dalton Trans.* **2012**, *41*, 9033–9045; e) M. A. Dureen, D. W. Stephan, *J. Am. Chem. Soc.* **2010**, *132*, 13559–13568.
- [4] M. F. Silva Valverde, E. Theuergarten, T. Bannenberg, M. Freytag, P. G. Jones, M. Tamm, *Dalton Trans.* **2015**, *44*, 9400–9408.
- [5] a) M. Radius, F. Breher, *Chem. Eur. J.* **2018**, *24*, 15744–15749; b) M. Radius, E. Sattler, H. Berberich, F. Breher, *Chem. Eur. J.* **2019**, *25*, 12206–12213.
- [6] D. Muz, K. Meyer, *Nat. Chem. Rev.* **2021**, *5*, 422–439.
- [7] T. Nishinaga, Y. Izukawa, K. Komatsu, *J. Am. Chem. Soc.* **2000**, *122*, 9312–9313.
- [8] N. Kramer, H. Wadeppohl, L. Greb, *Chem. Commun.* **2019**, *55*, 7764–7767.
- [9] a) T. Müller, R. West, *Adv. Organomet. Chem.* **2005**, *53*, 155–216; b) V. Y. Lee, A. Sekiguchi, *Acc. Chem. Res.* **2007**, *40*, 410–419; c) L. Greb, *Chem. Eur. J.* **2018**, *24*, 17881–17896.
- [10] a) A. Schulz, A. Villinger, *Angew. Chem. Int. Ed.* **2012**, *51*, 4526–4528; *Angew. Chem.* **2012**, *124*, 4602–4604; b) J. Y. Corey, *J. Am. Chem. Soc.* **1975**, *97*, 3237–3238; c) J. B. Lambert, Y. Zhao, *Angew. Chem. Int. Ed.* **1997**, *36*, 400–401; *Angew. Chem.* **1997**, *109*, 389–391; d) J. B. Lambert, Y. Zhao, H. Wu, W. C. Tse, B. Kuhlmann, *J. Am. Chem. Soc.* **1999**, *121*, 5001–5008; e) H. F. Klare, M. Oestreich, *Dalton Trans.* **2010**, *39*, 9176–9184; f) T. Stahl, H. F. T. Klare, M. Oestreich, *ACS Catal.* **2013**, *3*, 1578–1587; g) H. Großekappenberg, M. Reißmann, M. Schmidtman, T. Müller, *Organometallics* **2015**, *34*, 4952–4958; h) T. A. Engesser, M. R. Lichtenhaler, M. Schleep, I. Krossing, *Chem. Soc. Rev.* **2016**, *45*, 789–899; i) I. Mallov, A. J. Ruddy, H. Zhu, S. Grimme, D. W. Stephan, *Chem. Eur. J.* **2017**, *23*, 17692–17696; j) H. F. T. Klare, L. Albers, L. Süsse, S. Keess, T. Müller, M. Oestreich, *Chem. Rev.* **2021**, *121*, 5889–5985; k) D. Tanaka, A. Konishi, M. Yasuda, *Chem. Asian J.* **2021**, *20*, 3118–3123; l) H. Schmidt, S. Keitemeyer, B. Neumann, H.-G. Stammer, W. W. Schoeller, P. Putzi, *Organometallics* **1998**, *17*, 2149–2151; m) T. Müller, *Silicon Chem.* **2007**, *3*, 123–130; n) T. A. Kochina, D. L. Myalochkin, V. V. Avrorin, E. N. Sinotova, *Russ. Chem. Bull.* **2016**, *65*, 597–620; o) F. Diab, F. S. W. Aicher, C. P. Sindlinger, K. Eichele, H. Schubert, L. Wesemann, *Chem. Eur. J.* **2019**, *25*, 4426–4434; p) J.-J. Maudrich, F. Diab, S. Weiß, M. Zweigart, K. Eichele, H. Schubert, R. Müller, M. Kaupp, L. Wesemann, *Chem. Eur. J.* **2021**, *27*, 4691–4699.
- [11] C. Mohapatra, H. Darmandeh, H. Steinert, B. Mallick, K.-S. Feichtner, V. H. Gessner, *Chem. Eur. J.* **2020**, *26*, 15145–15149.
- [12] O. I. Kolodiazny, *Tetrahedron* **1996**, *52*, 1855–1929.
- [13] A. Sarbajna, V. S. V. S. N. Swamy, V. H. Gessner, *Chem. Sci.* **2021**, *12*, 2016–2024.
- [14] a) J. Escudié, C. Couret, H. Ranaivonjatovo, *Coord. Chem. Rev.* **1998**, *178–180*, 565–592; b) L. E. Gusel'nikov, *Coord. Chem. Rev.* **2003**, *244*, 149–240; c) H. Ottosson, P. G. Steel, *Chem. Eur. J.* **2006**, *12*, 1576–1585; d) H. Ottosson, A. M. Eklöf, *Coord. Chem. Rev.* **2008**, *252*, 1287–1314; e) K. M. Baines, *Chem. Commun.* **2013**, *49*, 6366–6369; f) K. K. Milnes, L. C.

- Pavelka, K. M. Baines, *Chem. Soc. Rev.* **2016**, *45*, 1019–1035; g) C. Weetman, *Chem. Eur. J.* **2021**, *27*, 1941–1954.
- [15] H. J. Bestmann, *Chem. Ber.* **1962**, *95*, 58–63.
- [16] R. Köster, D. Simić, M. A. Grassberger, *Liebigs Ann. Chem.* **1970**, *739*, 211–219.
- [17] N. Wiberg, *Lehrbuch der Anorganischen Chemie*, 102. Auflage, De Gruyter, Berlin, **2008**.
- [18] P. Pyykkö, M. Atsumi, *Chem. Eur. J.* **2009**, *15*, 186–197.
- [19] H. Grützmacher, H. Pritzkow, *Organometallics* **1991**, *10*, 938–946.
- [20] a) A. Maercker, *Angew. Chem. Int. Ed.* **1987**, *26*, 972–989; *Angew. Chem.* **1987**, *99*, 1002–1019; b) D. Y. Curtin, S. Leskowitz, *J. Am. Chem. Soc.* **1951**, *73*, 2630–2633.
- [21] N. Nakata, N. Takeda, N. Tokitoh, *J. Am. Chem. Soc.* **2002**, *124*, 6914–6920.
- [22] N. Nakata, N. Takeda, N. Tokitoh, *Organometallics* **2001**, *20*, 5507–5509.
- [23] a) C. Couret, J. Escudie, J. Satge, M. Lazraq, *J. Am. Chem. Soc.* **1987**, *109*, 4411–4412; b) M. Lazraq, J. Escudié, C. Couret, J. Satgé, M. Dräger, R. Dammel, *Angew. Chem. Int. Ed.* **1988**, *27*, 828–829; *Angew. Chem.* **1988**, *100*, 885–887; c) D. Ghereg, H. Gornitzka, H. Ranaivonjatovo, J. Escudié, *Dalton Trans.* **2010**, *39*, 2016–2022.
- [24] H. Meyer, G. Baum, W. Massa, A. Berndt, *Angew. Chem. Int. Ed.* **1987**, *26*, 798–799; *Angew. Chem.* **1987**, *99*, 790–791.
- [25] C. C. J. Escudie, H. Ranaivonjatovo, G. Anselme, G. Delpon-Lacaze, M. A. Chaubon, A. Kandri-Rodi, J. Satgé, *Main Group Met. Chem.* **1994**, *17*, 33–53.
- [26] A. Kawachi, Y. Tanaka, K. Tamao, *Organometallics* **1997**, *16*, 5102–5107.
- [27] a) E. D. Glendening, C. R. Landis, F. Weinhold, *J. Comput. Chem.* **2013**, *34*, 1429–1437; b) T. Lu, F. Chen, *J. Comput. Chem.* **2012**, *33*, 580–592.
- [28] a) U. Mayer, V. Gutmann, W. Gerger, *Monatsh. Chem.* **1975**, *106*, 1235–1257; b) M. A. Beckett, G. C. Strickland, J. R. Holland, K. S. Varma, *Polymer* **1996**, *37*, 4629–4631; c) H. GroBekappenberg, M. Reißmann, M. Schmidtmann, T. Müller, *Organometallics* **2015**, *34*, 4952–4958.
- [29] J. A. Cooke, C. E. Dixon, M. R. Netherton, G. M. Kollegger, K. M. Baines, *Synth. React. Inorg. Met.-Org. Chem.* **1996**, *26*, 1205–1217.
- [30] F. Forster, T. T. Metsänen, E. Irran, P. Hrobárik, M. Oestreich, *J. Am. Chem. Soc.* **2017**, *139*, 16334–16342.
- [31] N. A. Yakelis, R. G. Bergman, *Organometallics* **2005**, *24*, 3579–3581.
- [32] a) F. Neese, *WIREs Comput. Mol. Sci.* **2018**, *8*, e1327; b) F. Neese, *WIREs Comput. Mol. Sci.* **2012**, *2*, 73–78.
- [33] a) F. Weigend, R. Ahlrichs, *Phys. Chem. Chem. Phys.* **2005**, *7*, 3297–3305; b) O. Treutler, R. Ahlrichs, *J. Chem. Phys.* **1995**, *102*, 346–354.
- [34] J. Tao, J. P. Perdew, V. N. Staroverov, G. E. Scuseria, *Phys. Rev. Lett.* **2003**, *91*, 146401.
- [35] K. Eichkorn, F. Weigend, O. Treutler, R. Ahlrichs, *Theor. Chem. Acc.* **1997**, *97*, 119–124.
- [36] E. D. Glendening, C. R. Landis, F. Weinhold, *WIREs Comput. Mol. Sci.* **2012**, *2*, 1–42.
- [37] M. Frisch *et al.*, *Gaussian 09, Revision D.01*, Gaussian, Inc., Wallingford CT, **2016**.
- [38] T. A. Keith, *AIMAll (Version 19.10.12) D.01*, TK Gristmill Software, Overland Park, KS, USA, **2019** (<https://www.aim.tkgristmill.com>).

Manuscript received: November 3, 2021

Accepted manuscript online: November 24, 2021

Version of record online: December 9, 2021